A Co-factor matrix of the Hessian

Given a 3D scalar function $f : \mathbb{R}^3 \to \mathbb{R}$ we will use the notation f_{xy} to denote the partial derivative $\frac{\partial}{\partial x}\frac{\partial f}{\partial y}$ and the notation f_{xx} to denote the second derivative along x, i.e. $\frac{\partial^2 f}{\partial x^2}$ and so forth. Using these notations a Hessian matrix $\mathbf{H}$ can be written as the following:

$$\mathbf{H} = \begin{bmatrix} f_{xx} & f_{xy} & f_{xz} \\ f_{xy} & f_{yy} & f_{yz} \\ f_{xz} & f_{yz} & f_{zz} \end{bmatrix}$$

The co-factor of the Hessian, denoted by $\mathbf{H}_c$, is another matrix where every element is replaced by the co-factor of the corresponding element in $\mathbf{H}$, and the simplification is given below:

$$\mathbf{H}_c = \begin{pmatrix} f_{yy}f_{zz} - f_{yz}f_{yz} & f_{yz}f_{xz} - f_{xy}f_{zz} & f_{xy}f_{yz} - f_{yy}f_{xz} \\ f_{xz}f_{yz} - f_{xy}f_{zz} & f_{xx}f_{zz} - f_{xz}f_{xz} & f_{xy}f_{xz} - f_{xx}f_{yz} \\ f_{xy}f_{yz} - f_{xz}f_{yy} & f_{xy}f_{xz} - f_{xx}f_{yz} & f_{xx}f_{yy} - f_{xy}f_{xy} \end{pmatrix}$$

B Gaussian and Mean Curvature

Gaussian Curvature G is given by the following

$$\begin{aligned} G = \frac{1}{\|\nabla f\|^4}\Big[& f_x^2\left(f_{yy}f_{zz} - f_{yz}^2\right) + 2f_yf_z\left(f_{xz}f_{xy} - f_{xx}f_{yz}\right) + \\ & f_y^2\left(f_{xx}f_{zz} - f_{xz}^2\right) + 2f_xf_z\left(f_{yz}f_{xy} - f_{yy}f_{xz}\right) + \\ & f_z^2\left(f_{xx}f_{yy} - f_{xy}^2\right) + 2f_xf_y\left(f_{xz}f_{yz} - f_{zz}f_{xy}\right)\Big] \end{aligned}$$

and the Mean Curvature K is given by

$$\begin{aligned} K = \frac{1}{2\|\nabla f\|^3}\Big[& 2f_yf_zf_{yz} - f_x^2\left(f_{yy} + f_{zz}\right) + \\ & 2f_xf_zf_{xz} - f_y^2\left(f_{xx} + f_{zz}\right) + \\ & 2f_xf_yf_{xy} - f_z^2\left(f_{xx} + f_{yy}\right)\Big] \end{aligned}$$

where the gradient magnitude is $\|\nabla f\| = \sqrt{f_x^2 + f_y^2 + f_z^2}$.

C Empirical Analysis of Stability and Convergence

For this analysis we only varied Δt for each diffusion experiment keeping all the other parameters the same. Let $L_2(i,j)$ denote the l_2 norm between the volumes $f(\mathbf{x},i)$ and $f(\mathbf{x},j)$ at iterations i and j respectively during the evolution. This is given by the following:

$$L_2(i,j) = \sqrt{\sum_{\mathbf{x}\in\mathbb{R}^3}\left(f(\mathbf{x},i) - f(\mathbf{x},j)\right)^2} \tag{1}$$

The *Root Mean Squared Difference* RMSD between two volumes at iterations i and j, which is just the scaled l_2 norm, can now be given by:

$$RMSD(i,j) = \frac{L_2(i,j)}{\sqrt{V}} \tag{2}$$

where V is the total number of voxels and is a constant for a given dataset. Considering the volume $f(\mathbf{x},n)$ as a V dimensional point in $\mathbb{R}^V$, the RMSD can be thought of as the *Euclidean distance* between the volume at iterations i and j but only scaled by a constant $1/\sqrt{V}$.

We define a quantity $D(n)$, that measures the RMSD of the volume at iteration $n \in \{0\ldots N\}$ from the original volume, i.e. $f(\mathbf{x},0)$ as given below:

$$D(n) = RMSD(n,0) = \frac{L_2(n,0)}{\sqrt{V}} \tag{3}$$

Finally we define the rate of change of the *Euclidean distance*, scaled by the constant $1/\sqrt{V}$, with respect to time t between two successive volumes at iterations $n-1$ and n by the following:

$$S(n) = \frac{RMSD(n,n-1)}{\Delta t} = \frac{L_2(n,n-1)}{\Delta t\sqrt{V}} \tag{4}$$

Note that the quantity $S(n)$ is nothing but a numerical approximation of the instantaneous *speed*, scaled by the $1/\sqrt{V}$, of the evolution of the volume $f(\mathbf{x},n) \in \mathbb{R}^V$ at iteration n.

Now, for every Δt we ran N iterations of diffusion on a dataset and measured $D(n)$ and $S(n)$. The quantity $D(n)$ will show how a volume evolves with respect to the original volume in an l_2 norm sense and as well provide evidence of de-noising, which we will show later. On the other hand $S(n) \to 0$ as $n \to \infty$ will provide evidence of convergence of our proposed PDE.

We used a simulated structural MR data, obtained from the BrainWeb database (http://mouldy.bic.mni.mcgill.ca/brainweb/) for this study. This data is noise free yet realistic with many details and variation. Therefore, it is a good candidate for our test scenario. The structural MR data contains 256 gray levels and has a size of $181 \times 217 \times 181$.

In the first phase of the experiment we kept all the parameters the same as Section 6 of the paper and only varied Δt. Therefore, the other parameters were: $\lambda = 2$, $\sigma = 1$, $\rho = 1$ (in voxel units) and voxel spacing was assumed to be 1 in all directions and scalar values, which ranged between $(0,255)$. The 3D volumes were not scaled and a simple central differencing 2-EF filter-set was applied for all the derivative estimations.

For each Δt we ran $N = 25$ iterations. Figure 2 plots $D(n)$ and $S(n)$ for different values of Δt as indicated by the legend. With the noise-free MRI data, Figure 2b shows that for $\Delta t \leq 0.4$ the PDE behaves well. However for $\Delta t \geq 0.5$, the *speed* $S(n)$ drops less quickly until $\Delta t \geq 0.55$ when the PDE becomes unstable. However, the plot for $D(n)$ (Figure 2a) does not reveal anomalies until $\Delta t \geq 0.6$.

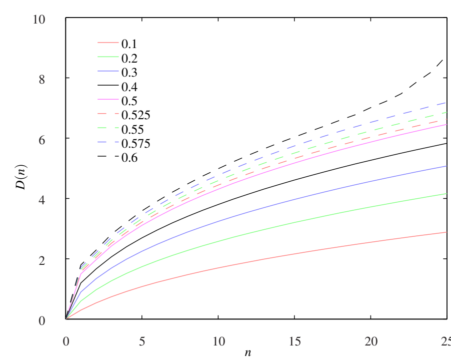

(a) $D(n)$

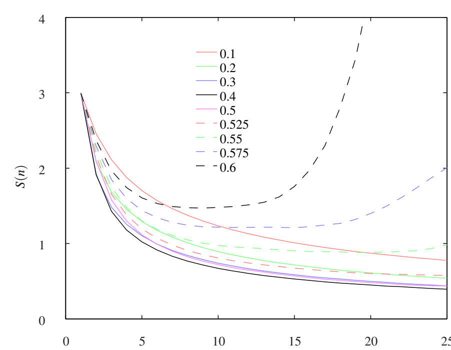

(b) $S(n)$

Fig. 2: Plot of (a) $D(n)$ and (b) $S(n)$ for each Δt (indicated by the legend), with the noise-free MRI data.

In the second phase of the experiment we added Gaussian noise with zero mean and a variance of 0.01 (in a normalized scale) to the synthetic MR data to add random high frequency variation to pose a more challenging test for our proposed diffusion PDE in terms of stability. This noisy volume has an SNR of 11.3056 dB. All other pa-

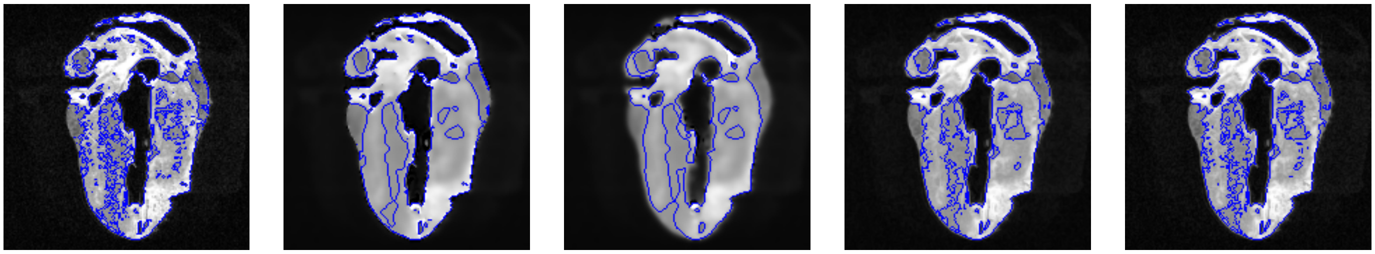

(a) Original (b) KM method: $k = 40$ (c) KM method: $k = 80$ (d) Our method: $\sigma = 1$ (e) Our method: $\sigma = 10$

Fig. 1: The 2D slice ($z = 65$) of the Sheep's Heart dataset, after diffusing with the KM method and our method as used in Figure 4 of the paper. We have also marked the same iso-surface of 153, as used in Figure 4 of the paper, with blue lines.

rameters were kept the same. For this experiment $D(n)$ was measured from the original noise-free MRI data. In Figure 3a, the slope of $D(n)$ is negative initially because the $D(n)$ was measured from the original noise-free MRI data and diffusion would bring the noisy data closer to the original in an l_2 sense with each iteration, i.e. the l_2 norm would progressively get reduced. This is an indication of de-noising taking place. This time however, both Figure 3a and Figure 3b indicate that for $\Delta t \geq 0.55$ the PDE becomes unstable. It is noteworthy that even a bad SNR of 11.3056 dB did not drastically change the stability from the one we found with the noise-free MRI data.

Finally, in the third phase, we used a $40 \times 40 \times 40$ data volume of a random signal uniformly distributed for values in $(0, 255)$. This poses an even more challenging test of stability and convergence. Figure 4b shows that even in the case of this random noisy volume the stability of the PDE did not change for $\Delta t < 0.55$. For $0.4 < \Delta t < 0.55$, although the PDE eventually converged, Figure 4a reveals some oscillation in $D(n)$ in the first few iterations.

In all three experiments, the plot of $S(n)$ showed that the PDE converged for $\Delta t \leq 0.4$ with $\Delta t = 0.4$ yielding the fastest convergence. On the other hand, the plot of $D(n)$ in all three experiments revealed that for $\Delta t \leq 0.4$ the PDE evolves without any oscillation. This led us to believe that for the parameter settings used in the paper, augmented with $\rho = 1$, our proposed PDE is stable for $\Delta t \leq 0.4$ for most practical purposes.

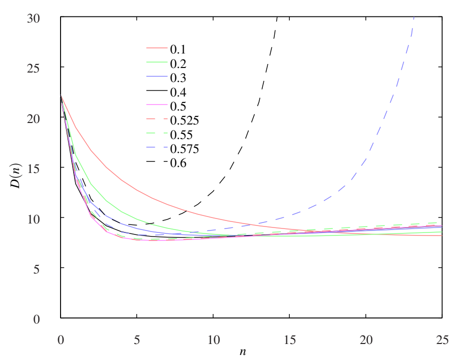

(a) $D(n)$

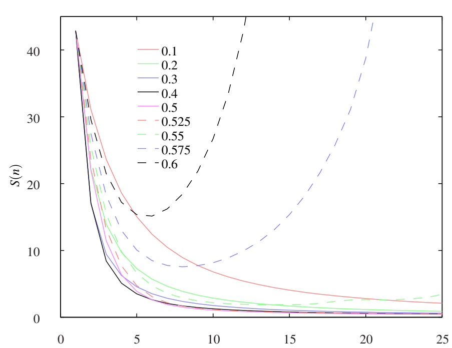

(b) $S(n)$

Fig. 3: Plot of (a) $D(n)$ and (b) $S(n)$ for each Δt (indicated by the legend), with the MRI data corrupted with the Gaussian noise.

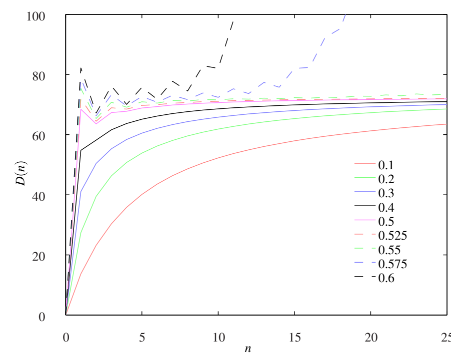

(a) $D(n)$

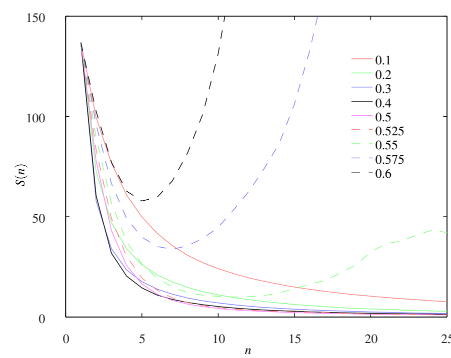

(b) $S(n)$

Fig. 4: Plot of (a) $D(n)$ and (b) $S(n)$ for each Δt (indicated by the legend), with a random data volume ($40 \times 40 \times 40$) uniformly distributed for $(0, 255)$.

D 2D Slice of Sheep's Heart with Iso-surface Marking

Figure 1 shows 2D slices of the Sheep's Heart dataset after diffusing it with our method and the KM method as described in the paper. These slices were taken from the 3D volumes as shown in Figure 4 of the paper and the same iso-surface of 153 is marked with blue lines. Figure 1 demonstrates that our method is more robust with its parameter σ compared to the gradient based KM method. A closer inspection into the "inside" of the iso-surface reveals that our method preserves structures better.